A98-31657

ICAS-98-5,9,4

PROBABILISTIC APPROACH FOR DESIGN OF A COMPOSITE RPV WING

K.A.Jacob, V.Prabhakaran, P.M.Saravanan and K.Rajaiah

Aeronautical Development Establishment, C.V.Raman Nagar,

Bangalore - 560 093, India.

Abstract

The Probabilistic approach is used in design of a composite wing for a remotely piloted vehicle (RPV). The loads encountered during launch, flight and recovery phases of the aircraft has been analysed. The varied conditions of loading make it difficult to go by the maximum load conditions and fixed factor of safety concept. The probabilistic approach quantified by an additional factor of safety is employed for design. The orthotropic material design and the concept of isotropic compliance criteria for arriving at material orthotropy based on the polar diagram of forces is proposed. The estimation of material allowables and a method for controlling the scatter based on sensitivity analysis is suggested. A multi design criteria based on strength, ' frequency and deformation limits is employed for the wing design. Finite Element Model analysis is carried out on selected structural configurations to arrive at the optimum design for minimum weight and to verify the design performance against the multi design criteria.

Introduction

The RPV considered here has a rectangular cross section fuselage, constant chord wing with aspect ratio around ten, twin boom tail configuration and pusher propeller. (Fig.1) [1].

The airframe is subjected to launch, flight and recovery loads. The launch and recovery mechanisms are different in different applications. The navel application prefer zero length launch with rocket booster and recovery on board ship with the help of a travelling net. The army require a hydro pneumatic catapult launch from rails and parachute aided recovery. Other land based civil and military operations make use of conventional take off and landing from runway. The RPV is also used as a platform for various payload combinations and fly for different duration depending on mission requirements and the all up weight of RPV vary upto 20 percent.

The design of fuselage has many common features, however, depending on the mechanism of launch and recovery, modifications are made. For example, landing gear is required for runway operations and suitable interfaces are required for rail launch and rocket assisted launch operations. For parachute assisted recovery, the para deployment and attachments as well as landing gas bag housing and inflation mechanisms are required. Considering these facts, the fuselage is developed as different versions as per requirement.

Mean while, the possibility of employing common wing and empennage modules for all the versions is studied. The present exercise is to develop a methodology for design of the wing considering the various load conditions encountered in different versions of the RPV, based on a probabilistic approach.

Composite Application

At present, composite materials are being used in primary structures of the airframe such as wing, fuselage and control surfaces.

The maximum advantage of composite application can be obtained by providing for their usage in an airframe structure as early as possible in the preliminary stage of the aircraft design process.

The composites have the capability of directed change of their properties in compliance with structural assignments. The material design call for tailoring of the material layers depending on the stiffness and strength requirements. Simultaneously achieving the orthotropic structural design as well as designing the material combination and layer sequence and ensuring required reliability, is of considerable importance.

Loads

In compliance with the airworthiness standards, the designer must state the expected conditions of aircraft operation and establish flight and other operational parameters with an indication of limiting operational conditions, flying characteristics, controllability and stability characteristics. Based on these parameters the load spectrum is derived and design criteria are evolved.

Flight loads

The RPV is subjected to launch,flight and recovery loads. The flight loads are estimated and the velocity load factor (v-n) diagram is given in Fig 2. The maximum load occurs when the aircraft is held against heavy gust (25 m/sec) in bearing and altitude, in the autonomous mode. The upgust is more critical from wing loading point of view. The load distribution along the span is elliptical and center of pressure falls around 25 percent of chord. Due to eccentricity of loading the wing is also subjected to varying torsional moments along the span (Fig 3.). In the particular case considered the tail booms are attached to the wing and the tail loads are producing additional torsion and bending of the wing. The aerodynamic drag as well as aileron loads also act on the wing which are superposed over the main loads.

Launch loads

The mechanism of take off are

a. conventional take off from runway
b. rail launch (hydropneumatic catapult or rocket)
c. zero length rocket assisted launch

During conventional take off, the wing is loaded by inertia loads due to forward acceleration and buildup of lift with speed.

During rail launch the inertia loads act in the plane of the wing and which is, mass of the wing multiplied by the acceleration (10g). The lift load buildup as the speed increases to launch speed of 40 m/sec.

In the zero length launch, the launch acceleration is limited to 8g level, since it causes biaxial loading on wing and to take care of the variation in thrust due to temperature and other variations.

The inertia loads are nearly elliptical loading based on the distribution of mass of wing from root to tip. The loads in plane and out of plane of the wing are considered. These loads are combined with aerodynamic lift loads at the end of launch. These loads are generally less than the critical flight load considered (4g).

Recovery Loads

The recovery conditions are

a. conventional landing on runway with cable arrester
b. parachute deployment loads (8.5g)
c. land impact load with gas bags (10g)
d. net recovery loads (3g)

During conventional landing the cable arrester is adjusted to give a retardation less tan 5g.

The parachute deployment loads are limited to 8.5g considering the possible variations during deployment.

The land impact loads with gas bags are limited to 10g. The inertia loads are given by the mass of the wing multiplied by the deceleration levels.

The net recovery employ a vertical travelling net which retard the forward velocity of the net and a horizontal net which prevent the vertical fall of the RPV. For wing, the net recovery loads are critical, considering the fact that the total inertia loads (mass of aircraft multiplied by deceleration level) are reacted on the wing as uniformly distributed load and produce bending moments more than that due to flight loads. The attitude of aircraft change during net impact and the loads have to be resisted by wing, in plane , out of plane or combined mode. The horizontal net produces heavy bending of wing , during secondary impact (Fig 4 and 5).

Deformation Analysis Program

Structural Configuration

The structural configuration applicable to the combination of load and structural depths considered may be thought of as a particular type of external surface, or wing skin, which is well over half the weight of the 'basic structure', working with a particular type of internal structure (a specific arrangement of ribs and spars, full depth core etc.). The initial configuration is checked for the bending moment, beam shear and torsional moment resulting from the critical load condition.

The structural design criteria for upper and lower skin panels include compression buckling failure or compression yield, tension allowable or allowable fatigue stress whichever is critical. The optimum relationship between the skin panel material and supporting structure spacing is determined by standard structural analysis with in the program.

The spar web thickness is determined from consideration of buckling due to shear loading in the box beam. The spar flange width is determined from consideration of the adhesive shear allowable.

A deformation analysis is executed with the initially selected configuration to obtain skin loads and which in turn will be utilised in the material design of the skin.

Deformation Analysis

The wing structure is considered as an unsymmetrical cantilever plate with bending stiffness varying as a function of x and y, the differential equation for deflection can be expressed in the invariant form as

$$\nabla^2(D\nabla^2 w) - (1-\nu)\Diamond^4(D,w) = q + q^1 \text{..(1).}$$

where $\Diamond^4(D,w) =$

$$\frac{1}{2}\left\{(\nabla^2 w(\nabla^2\theta) + \nabla^2(w\nabla^2\theta + \theta\nabla^2 w)\right\}$$

$$-\frac{1}{4}\left\{\nabla^4(w,\theta) + w\nabla^4\theta + \theta\nabla^4 w\right\}$$

q is the normal pressure and q^1 is the equivalent additional pressure which replaces the effect of middle surface forces on deflection [2].

The deflection at any point can be expresses as a sum of two components as follows (Fig. 6)

$$w(x,y) = \bar{w}(x) + \sum_{i=1}^{N} c_i y_i \theta(x) \quad \text{.....(2)}$$

$\bar{w}(x)$ is the deflection of the plate at any point on x axis and $\theta(x)$ is the rotation of the line x = constant at the corresponding point. Then equation (1) reduces to two coupled differential equations

$$\frac{\partial^2}{\partial x^2}\left(a_1\frac{\partial^2 \overline{w}}{\partial x^2}+a_2\frac{\partial^2\theta}{\partial x^2}\right)-p_1=0 \quad \text{.....(3)}$$

$$\frac{\partial^2}{\partial x^2}\left(a_2\frac{\partial^2 \overline{w}}{\partial x^2}+a_3\frac{\partial^2\theta}{\partial x^2}\right) - 2(1-\nu)\frac{\partial}{\partial x}\left(a_1\frac{\partial\theta}{\partial x}\right)-p_2=0 \quad \text{.....(4)}$$

The boundary conditions are

$$\left[w=\frac{\partial .\overline{w}}{dx}=\theta=\frac{\partial\theta}{dx}\right]_{x=0}=0$$

$$\left[a_1\frac{d^2w}{dx^2}+a_2\frac{d^2\theta}{dx^2}\right]_{x=l}=0$$

$$\left[\frac{d}{dx}\left(a_1\frac{d^2\overline{w}}{dx^2}+a_2\frac{d^2\theta}{dx^2}\right)\right]_{x=l}=0 \quad \text{.....(5)}$$

$$\left[a_2\frac{d^2\overline{w}}{dx^2}+a_3\frac{d^2\theta}{dx^2}\right]_{x=l}=0$$

$$\frac{d}{dx}\left(a_2\frac{d^2\overline{w}}{dx^2}+a_3\frac{\partial^2\theta}{dx^2}\right) -2(1-\nu)a_1\left[\frac{d\theta}{dx}\right]_{x=l}=0$$

The stiffness terms a_1, a_2, a_3 and p_1, p_2 are obtained by integrating along the chord direction corresponding to respective stations.

$$a_1=\int_{t_1(x)}^{t_2(x)}D\,dy \quad ; \quad a_2=\int_{t_1(x)}^{t_2(x)}D\,y\,dy$$

$$a_3=\int_{t_1(x)}^{t_2(x)}D\,y^2\,dy \quad \text{.....(6)}$$

$$p_1=\int_{t_1(x)}^{t_2(x)}q\,dy \; ; \; p_2=\int_{t_1(x)}^{t_2(x)}y\,q\,dy \quad \text{.....(7)}$$

p_1 represent the load per unit width acting on a chord section and p_2 represent the moment of the load p_1 about x axis. The recurrence relations derived for $\overline{w}$ and θ from the difference form of equations (3) and (4) are

$$\overline{w}_i=[-E_1w_{i-2}-E_2w_{i-1}-E_4w_{i+1}-E_5w_{i+2} -F_1\theta_{i-2}-F_2\theta_{i-1}-F_3\theta_i-F_4\theta_{i+1} -F_5\theta_{i+2}+p_1h^4]/E_3 \quad \text{.....(8)}$$

$$\theta_i=[-F_1w_{i-2}-F_2w_{i-1}-F_7w_i-F_8w_{i+1} -G_1\theta_{i-2}-G_2\theta_{i-1}-G_4\theta_{i+1} -G_5\theta_{i+2}+p_2h^4]/G_3 \quad \text{.....(9)}$$

where E_i are functions of a_1 and Fi are functions of a_2 and G_i are functions of a_1 and a_3 [3].

The equations (8) and (9) get modified near the boundaries conforming to boundary conditions (5)

Relations (8) and (9) contain both $\overline{w}$ and θ variables and hence can not be solved by elimination. Here an alternating direction relaxation method is employed. From eqn. (8) $\overline{w}$ values are obtained which maintains θ_i as the initial known values. The computed value of $\overline{w}_i$ are used in equation (9) to obtain new values of θ_i which are in turn used for the next iteration of (8). The iteration proceeds till sufficient convergence is obtained. The stress output from the deformation analysis are employed to calculate the skin loading at different stations corresponding to various loading cases.

Polar Load Diagrams and Critical Load Envelope

The stresses in the wing skin due to the different loading conditions obtained from deformation analysis are integrated over the skin thickness to obtain the skin loads at different stations (Fig. 7)

$$p_x=\int_{z_1}^{z_2}\sigma_x\,dz \quad ; \; p_y=\int_{z_1}^{z_2}\sigma_y\,dz$$

$$p_{xy}=\int_{z_1}^{z_2}\sigma_{xy}\,dz \quad \text{..... .....(10)}$$

The forces in the skin due to different critical loading conditions can be broken up into principal loads by using the Mohr's circle which will give the direction and intensity of principal loads (Fig. 8).

The principal loads are assembled into a polar diagram which will provide the critical load envelope. The critical load envelope vary from station to station. The envelope condition represent the maximum load at any angle which might be expected during the life time of the aircraft. Near the root sections, the bending is prevalent in x direction and hence the polar diagram will be a high aspect ratio ellipse (approximately) with major axis parallel to x axis. For outboard wing the torsional forces are comparable to the bending forces and hence the polar load diagram form an ellipse with relatively low aspect ratio. At the leading edge station the force directions are different depending on the wing geometry .

The laminate optimisation program then proceeds to orient and investigate different type of filamentary materials to select the material and orientation depending on the loading conditions set forth by the critical load envelope.[3]

Material Design - Laminate Properties

The constitutive relation (stress-strain) for an orthotropic laminate is

$$\begin{bmatrix}\sigma_1\\ \sigma_2\\ \tau_{12}\end{bmatrix} = \begin{bmatrix}S_{11} & S_{12} & 0\\ S_{12} & S_{22} & 0\\ 0 & 0 & S_{66}\end{bmatrix}\begin{bmatrix}\varepsilon_1\\ \varepsilon_2\\ \gamma_{12}/2\end{bmatrix} = S_k\,\varepsilon_o \quad \ldots(11)$$

$$S_{11} = \frac{E_{11}}{(1-\nu_{12}\nu_{21})}\,, \quad S_{22} = \frac{E_{22}}{(1-\nu_{12}\nu_{21})}$$

$$S_{12} = \frac{\nu_{21}E_{11}}{(1-\nu_{12}\nu_{21})}\,, \quad S_{66} = G_{12}$$

$$\nu_{21} = \frac{E_{22}\nu_{12}}{E_{11}}$$

The stiffness matrix elements with respect to the laminate reference axes x,y can be computed by

$$(\bar{S}_{ij})_k = T^{-1}S_kT \quad \ldots(12)$$

where T is the transformation matrix

The laminate stiffness properties can be obtained by summing up the stiffness terms [4]

$$A_{ij} = \sum_{k=1}^{n}(\bar{S}_{ij})_k(h_k - h_{k-1}) \quad \ldots(13)$$

Since the skin is subjected to axial stresses, for symmetrical laminates,

$$\varepsilon^o = A^{-1}N \quad \ldots(14)$$

Orthotropic Design - Isotropic Compliance Criteria

The stiffness critical design suggests similar compliances in all direction or isotropic compliance (load/stiffness = compliance) (Fig. 9). For an efficient design the laminate stiffness should be such that the resultant stiffness diagram is an ellipse with aspect ratio and orientation of major axis same as the nearest ellipse constructed enveloping the polar load diagram. This assures a symmetric compliance.

The strain should be limited to the limit strain ε_l which is less than ultimate strain ε_u by a factor r which is less than unity.

$$\varepsilon_l = r.\varepsilon_u \quad \ldots(16)$$

By employing a maximum strain criteria it is possible to determine the stiffness requirements of the laminate in different directions.

The laminate optimised for isotropic compliance have to be checked for local constraints, buckling, stress raisers, interlaminar shear and against strength

criteria. It is advisable to analyse in detail joints and load introduction through metallic inserts, and reduce the stress levels by additional thickness or suitable reinforcements. The interlaminar shear strength can be increased in critical areas by stitching the plies.

Design allowables

The design allowables are computed for the lamina based on test results for elastic modulii and strength properties. The design A and B values are given by

$$A = \bar{y} K_a S \quad \text{.....(17)}$$
$$B = \bar{y} K_b S$$

where $\bar{y} = \sum_{i=1}^{n} y_i / n$ (sample mean)

$$S = \sqrt{\sum_{i=1}^{n} (y_i - \bar{y})^2 / (n-1)}$$ (Standard deviation)

K_a = one sided tolerance limit factor corresponding to atleast 0.99 of a normal distribution and confidence coefficient of 0.95 from tabulated data (99 percent probability with 95 percent confidence)

K_b = 90 percent probability with 95 percent confidence.

The lamina properties with their variables are combined to give the laminate properties and their probability distribution (Fig 10). The lamina property variations are also computed with varying values of humidity and temperature. Fig 11 illustrate the durability and significance of design allowables. The lamina properties are combined to obtain the laminate properties. The variability of lamina properties are employed to estimate variations in the laminate properties. Design charts are produced which are useful in selecting the layup sequence.

The sample size required to obtain the A basis design values is large. Hence a smaller sample size is used and a tolerance factor is employed over the mean to obtain 95 percent confidence level.

Sample size n =	3	6	10	20	30
factor K=	0.67	0.75	0.80	0.9	1.0

Reliability and Sensitivity Analysis

The present approach is to assess the reliability of the design with respect to a given failure mode at any point of design. This is achieved by the method of statistical trials in combination with sensitivity analysis by variance separation (VS). The Monte Carlo Simulation (MCS) is very useful for the statistical trials.

Initial probability distributions are formulated for all variables which appear in the design reliability model of each failure mode.[5] Let y be the failure mode function of the independent variables x_1, x_2, x_3, then

$$y = f(x_1, x_2, x_3) \quad \text{.....(18)}$$

When the probability distribution of the variables are known or approximated then the MCS technique is used to generate the theoretical sample for y and also its probability distribution.

Sensitivity Analysis

The sensitivity analysis can be used to determine which of the variables are the most important for improving reliability. Sensitivity analysis is done using variance separation technique. The procedure is as follows.

1. It is assumed that y can represented as a linear function of the variables x_1, x_2 and x_3

$$y = c + b_1 x_1 + b_2 x_2 + b_3 x_3 + \ldots \quad \text{.....(19)}$$

where c, b_1, b_2 are unknown constants.

2. Evaluation of constants using regression method.
3. During the calculation of MCS histogram the standard deviation of each variable xi (σ_i) are also computed.
4. The coefficients bi together with σ_y and σ_i are used to determine the percentage variation (PV) in y which is caused by each xi.

$$PV(x_i) = 100 b_i^2 \frac{\sigma_i^2}{\sigma_y^2} \quad \text{.....(20)}$$

Multi - Design Criteria and Optimisation

Stiffness criteria The wing shall be stiff enough to satisfy the stiffness criteria defined as[6]

$$d_a / d > 1 \quad \text{.....(21)}$$

d = wing tip deflection
da = maximum tip deflection allowed

Frequency criteria The overall stiffness of the wing shall be such that coupling of control system and structural excitation does not take place. The frequency criteria is given by

$$\frac{f}{f_a} > 1 \quad \text{.....(23)}$$

f = fundamental frequency
fa = minimum fundamental frequency allowed
fa = 1.5 fc
fc = control system frequency

Stiffness Factor The stiffness factor is defined as

$$S_f = (d_a / d).(f / f_a) > 1 \quad \text{.....(24)}$$

Stress factor The stresses in the material should be within the acceptable limits. The tensile, compressive and shear stress factors are given as

$$(t_a / t) > 1 \quad \text{.....(25)}$$

t = tensile stress
t_a = maximum allowable tensile stress

$$(c_a / c) > 1 \quad \text{.....(26)}$$

c = compressive stress
c_a = maximum allowable compressive stress

$$(\tau_a / \tau) > 1 \quad \text{.....(27)}$$

τ = shear stress in wing section
τ_a = maximum allowable shear stress

Minimum Weight Criteria

Minimum weight criteria is stated as

$$Wm = (Wf \,.\, Sf \,.\, Uf - 1) \quad \text{.....(28)}$$

Wm = 0 is critical design
Wm = -ve is not acceptable design
Wm = +ve but minimum is taken as the best design
Wf = W/Ws
W = actual design weight
Ws = maximum specified design weight
Sf = Stiffness factor
Uf = material utilisation factor

$$U_f = \frac{b(n)d(n)\frac{h_t(n)t_a(n)}{N_1 t(n)} + \frac{h_c(n)c_a(n)}{N_2 c(n)} + H(n)d(n)\left\{\frac{h_s(n)\tau_a(n)}{N_3(n)} - \right\}}{b(n)d(n)\{h_t(n)h_c(n)\} + H(n)d(n)h_s(n)} \quad \text{..(29)}$$

where

b(n) = width of torque box
d(n) = rib spacing
ht(n) = skin thickness on tension side of torque box
hc(n) = skin thickness on compression side of torque box
hs(n) = thickness of shear web of spars
H(n) = web height of front and rear spars
N_1, N_2, N_3 = design factors
N_1 = load factor = n11.n12.n13
N_2 = environmental factor = n21.n22.n23
N_3 = fitting factot = n31.n32.n33

Finite Element Analysis

Based on the deformation analysis and orthotropic design the structural configuration and material design is arrived at. The configurations finally selected viz.,

a. stiffened skin configuration
b. full depth core construction
c. sandwich skin construction

have been analysed using FE analysis to check against the multi design criteria. The deflections, rotation, stresses and frequency have been computed for different combinations of loads. Density of materials used are given to get the self weight of the structure. Dynamic analysis has been performed using sub space iteration method to estimate the first natural frequency.

All the structural options are modelled using COSMOS/M 1.65a software code. The GFRP and CFRP material components are modelled as SHELL4 elements and C/GFRP hybrid material lements are modelled as SHELL4L composite elements. The foam core of sandwich skin is modelled as SOLID brick elements (Fig 12).

The laminate properties viz., elastic modulus, tensile strength, compressive strength, shear strength etc are fed as mean values and the variability in the material is accounted as reduced properties for sensitive variables. Wherever mean values are used, the sample size and variability are controlled by additional factors.

The analysis results are screened through the optimisation program to check for the multi design criteria and to rank the design for minimum weight (Table 1).

Results and conclusion

The design procedures based on the probabilistic approach has been tried out on the RPV wing. The wing has been analysed and optimised for minimum weight. The selected configuration has been manufactured and tested to verify the stresses, deformation and frequency requirements and were found to be acceptable.

The wing was flight testd several times and subjected to different load conditions of launch, flight and recovery loads (Plates 1 to 4). The wing has withstood all the load conditions successfully.

In certain cases, damages occured on the wing, during land impact, due to uneven ground and due to poor stability of gas bags under oblique impact. The damages were local and the wings were repaired and reflown. Damages were also noticed during net recovery trial landings. It was found that the deceleration level was 5g which was more than prescribed level (3g). This was also substantiated by strain gauge readings at the wing root. The travel of the net is being increased and stiffness of damper (water twister) reduced to limit the deceleration levels.

The probabilistic approach provide insight into the problem and the simulation (MCS)and sensitivity analysis are very useful tools for the designer of composite structures, where the material design and process variables are to be considered along with structural sizing.

The additional factor of safety concept is a practical and viable method provided the factors are selected considering the variability of material strength characteristics, the confidence on load predictions and amount of test carried out on specimens and structure. A margin of safety of minimum 20 percent shall be ensured at all times of operation.

The repaired and damaged wings were evaluated by load testing(linearity checks) upto limit loads and by frequency checks (and compare with earlier values) to ensure overall stiffness of wing.

It is concluded that the probabilistic approach is viable and important for high performance composite structures such as composite aircraft wing.

References

1. Jacob. K.A., et. al., "Mini RPV Airframe", Detailed Design Document, ADE, Bangalore, 1994
2. Mansfield,E.H., "The Bending and Stretching of Plates", Pergamon, 1964
3. Jacob.K.A., and C.Rajput,"Stiffness Critical Design with Composites", Design and Development in Aeronautics, Festschrift to Dr V.M.Ghatage, HAL, Bangalore, 1983
4. Nicholas,R., Composite construction Materials Handbook, Prentice Hall, 1976
5. Jacob,K.A., Prabhakaran,V., and Murthy,A.S.R., "A Computer Code for Structural Reliability Estimation", Annual Technical meeting,AeSI, Calcutta, 1990
6. Saravanan,P.M., et. al., "Optimisation studies on Composite Wing Structure", PICAST-3, Xian, China,1997

Acknowledgements

The authors are thankful to Dr KG Narayanan, Director and Grp Capt Babu Rao, Project Director, for their support and encouragement during the course of this work.

Structural Model	Deflection criteria	frequency criteria	Tensile stress factor	Comp stress factor	Shear stress factor	Stiffness factor	Material utilisation factor	Weight factor	Cost factor	Minimum weight criteria	Minimum cost criteria
Option 1 Case 1 Stiffened skin GFRP and Carbon tape	0.93	0.96	2.03	5.0	1.58	0.893	24.87	1.284	2.269	27.52	2.939
Option 1 Case 2 Stiffened skin CFRP, GFRP and Carbon tape	1.315	1.159	1.53	1.8	1.41	1.524	26.40	1.223	3.597	48.21	4.399
Option 2 Case 1 Stiffened skin CFRP and GFRP	1.844	1.65	2.22	3.81	1.50	3.043	17.94	0.882	8.667	47.15	7.644
Option 2 Case 2 Stiffened skin G/CFRP and GFRP	1.399	1.30	1.94	2.32	1.97	1.819	15.55	1.025	5.451	27.99	5.587
Option 3 Case 1 All Full depth sandwich skin CFRP, GFRP and R51 foam	1.298	1.138	1.79	2.58	1.50	1.477	23.71	1.004	7.629	34.16	7.659
Option 3 Case 2 All Full depth sandwich skin G/CFRP, GFRP and R51 foam	1.154	1.014	1.91	1.81	2.03	1.17	20.36	1.128	5.90	25.87	6.655
Option 4 Case 1 Sandwich skin CFRP, GFRP and R51 foam	1.389	1.374	1.79	2.76	1.37	1.908	5.46	0.803	8.379	7.37	6.728
Option 4 Case 2 Sandwich skin G/CFRP, GFRP and R51 foam	1.078	1.097	1.57	1.77	1.77	1.162	4.98	0.916	5.829	4.39	5.339

Table 1 THE OPTIMISATION PARAMETERS OF WING STRUCTURE

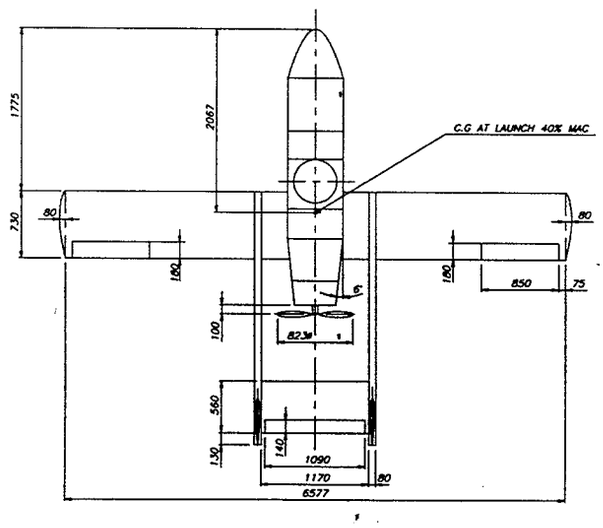

Fig 1 MODULAR RPV CONFIGURATION

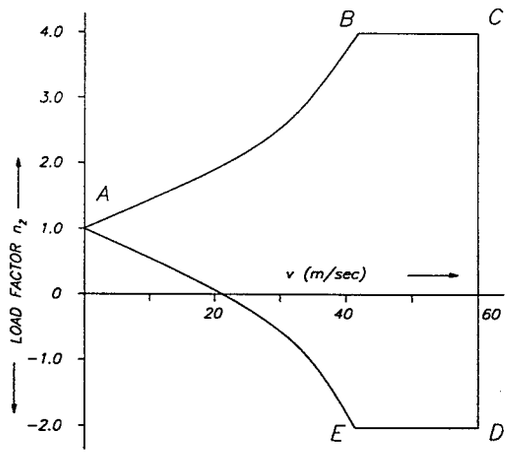

Fig 2 v–n DIAGRAM

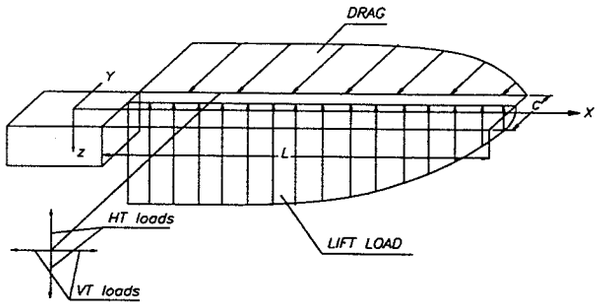

Fig 3 WING LOAD DISTRIBUTION

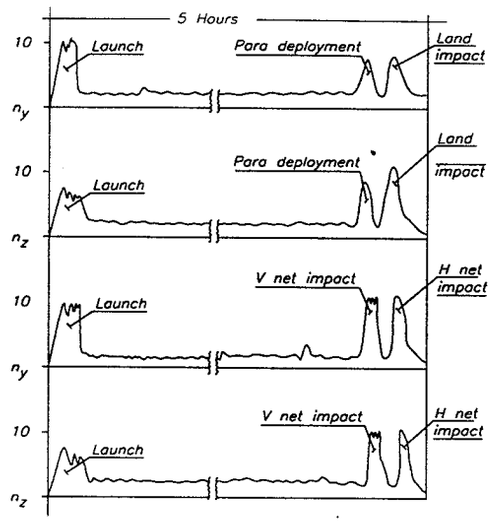

Fig 4 INERTIA LOADS

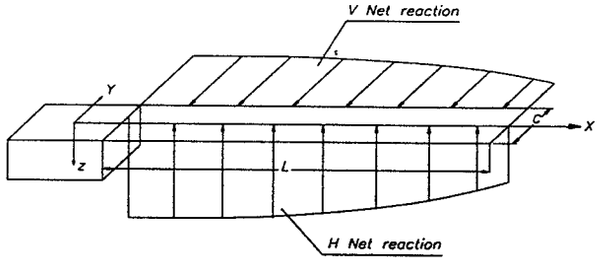

Fig 5 NET RECOVERY LOADS

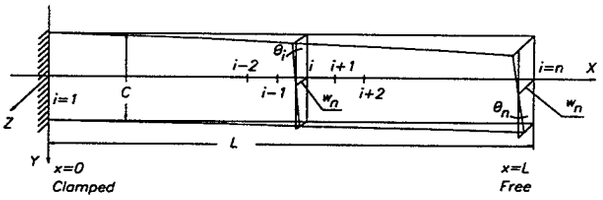

Fig 6 DEFORMATION OF WING

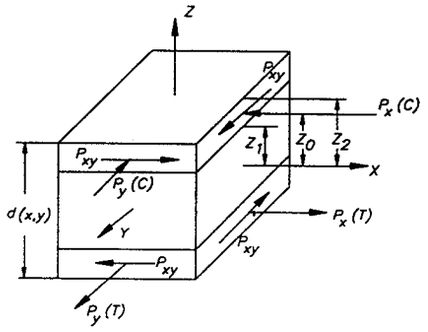

Fig 7 WING SKIN LOADING

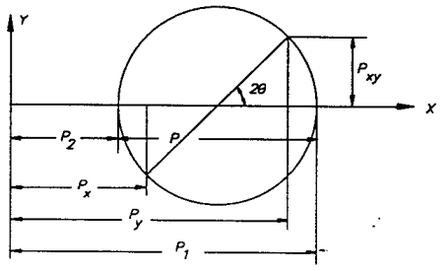

Fig 8 MOHR'S CIRCLE OF LOADS

$$\frac{a}{b} = \frac{a'}{b'} \quad \text{and} \quad \frac{P_\theta}{S_\theta} = \epsilon_\theta = \epsilon_o = \epsilon_1$$

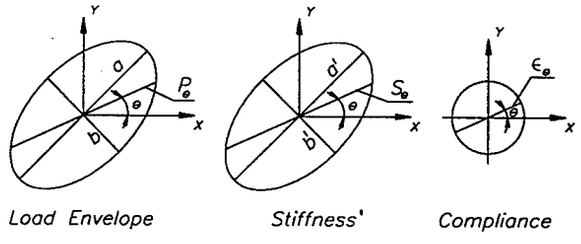

Fig 9 ISOTROPIC COMPLIANCE

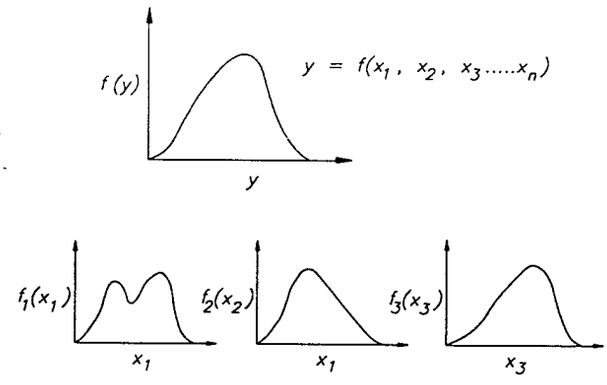

Fig 10 PROBABILISTIC DISTRIBUTION OF VARIABLES AND OBJECTIVE FUNCTION

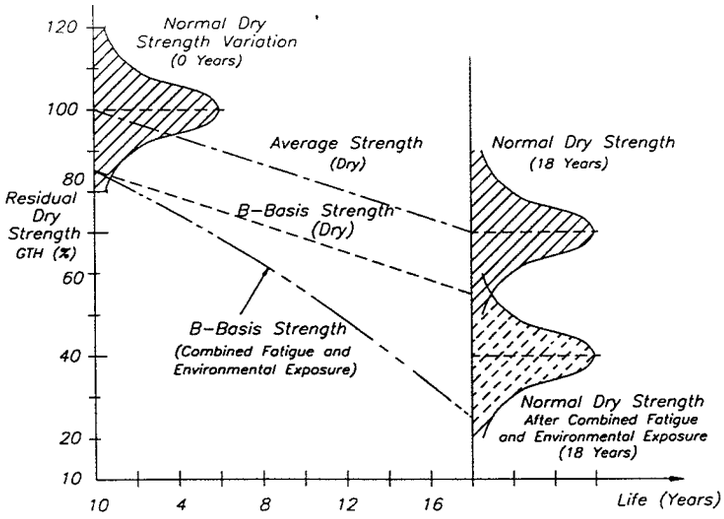

Fig 11 DURABILITY AND STRENGTH VARIATIONS

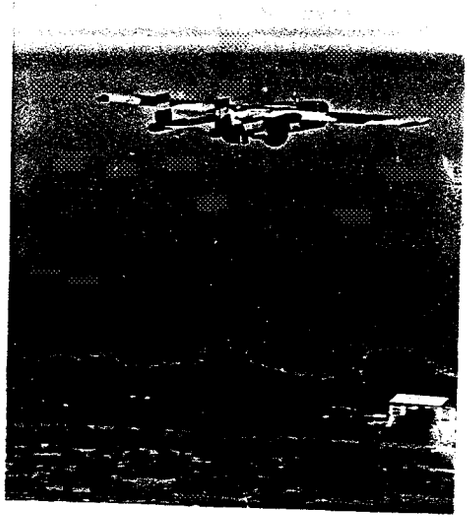

Plate 2 RPV IN FLIGHT

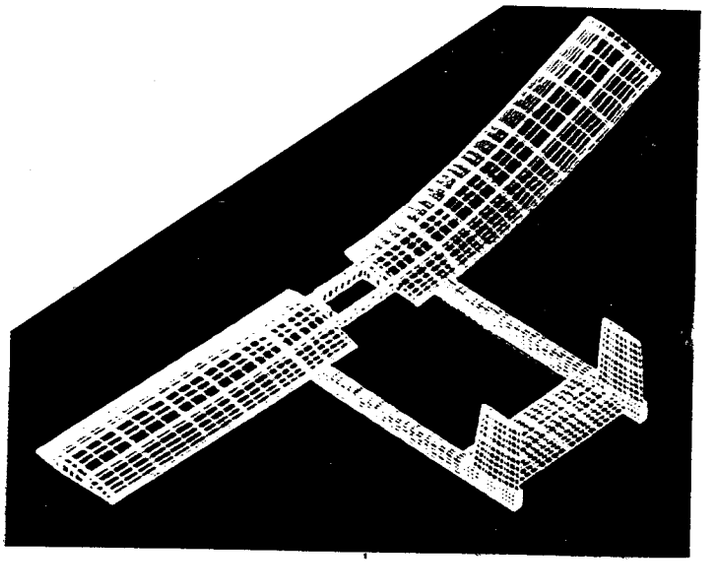

Fig 11 FINITE ELEMENT MODEL OF WING WITH TAIL AND BOOM

Plate 3 PARACHUTE AIDED RECOVERY

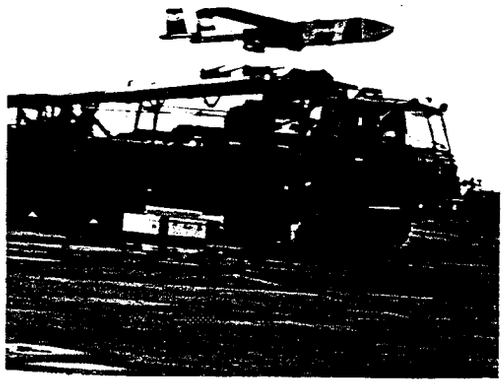

Plate 1 RPV LAUNCH FROM HYDRO PNEUMATIC LAUNCHER

Plate 4 RPV RECOVERY BY TRAVELLING NET